ISSN 1330-3651 (Print), ISSN1848-6339 (Online) https://doi.org/10.17559/TV-20240728001885
Original scientific paper

Dynamic Multi-Period Intelligent Traffic Allocation Based on Multi-Objective Data Mining

Zishuo CHEN, Jingfeng GUO*, Fengda ZHAO, Ruishan DU, Lingdong MENG

Abstract: This study develops a sophisticated dynamic, multi-period intelligent traffic allocation algorithm using multi-objective data mining techniques, designed to optimize the incorporation of renewable energy systems (RESs) and electric vehicles (EVs) within electrical power grids. Given the inherent intermittency and unpredictability associated with RESs and EVs, the algorithm utilizes Dynamic Optimal Network Reconfiguration (DONR) and Capacitor Bank Switching (CBS) to address these challenges effectively. This integrated approach aims to enhance grid stability and operational efficiency, focusing on reducing energy losses, improving voltage profiles, and achieving financial savings through optimized 24-hour grid operations. The core innovation of this research is the application of the Artificial Hummingbird Algorithm (AHA), which has been adapted for the first time to tackle this multi-faceted optimization problem. By considering the impacts of variable solar generation and the demands of diverse load profiles, including substantial EV penetrations, the AHA navigates complex decision spaces to find optimal solutions. This methodology was rigorously tested using an enhanced IEEE 33-bus benchmark system, where various scenarios were simulated to evaluate the computational effectiveness of the AHA compared to other prevailing methods. The results from these simulations clearly demonstrate the superior performance of the integrated DONR and CBS strategy, particularly in managing the dynamic and stochastic nature of load demands and renewable energy inputs in real-time scenarios. The method by dynamic reconfiguration may boost the overall savings to 6903.03 $/h and decrease inefficiencies at (87.95 kW + j64.72 kVAr).

Keywords: electrical power grid; electric vehicles; renewable energy system; traffic allocation algorithm

1 INTRODUCTION

Recently, there has been a global trend towards integrating clean energy sources (RESs) and adopting electric vehicles (EVs) as a means to promote energy efficiency and lower transportation-related pollution in order to fulfill the goals set by the UN, or SDGs [1]. Both forms of energy are anticipated to see explosive development in the near future, according to the Intergovernmental Identification Agency's (IEA) Worldwide EV Assessment 2022 [2] and the Internationally Electricity Agency's (IRENA) Clean Energy Stats 2022 [3]. Despite the fact that both of these methods are environmentally sustainable, their discontinuous and unpredictable nature makes monitoring and administering electricity networks more difficult nature [4, 5]. The ambiguity of Renewable Energy Sources (RESs) leads to a discrepancy between supply and demand, a decrease in reserve generation, and volatility in frequency. The integration of large-scale renewable energy systems (RESs) in power grids results in reduced system frequency stability due to low inertia. Due to the unpredictable nature of power output caused by fluctuating wind speed and sunlight intensity, the integration of renewable energy sources onto the electrical grid at a large scale may result in concerns related to the stability and dependability of the system [6, 7]. However, the growing penetration of electric vehicle (EV) charging leads to a rise in power consumption, energy asymmetry, higher losses, decreased voltage profile, reduced stability, and insecurity margins. These issues are significant problems in nearly all electrical distribution grids (EDNs) [8, 9]. A study conducted in Western Australia on an asynchronous electric vehicle (EV) charging time model found significant increases in transformer load and voltage abnormalities. These issues have the potential to surpass the capacity of the existing distribution equipment [10]. In these conditions, it has become crucial to utilize planning and functioning studies to enhance the capacities of generation, transmission, and distribution. Additionally, it is essential to integrate the best possible use of chargers for electric vehicles, regulated charging circumstances, batteries (ESSs), volt/VAr control optimization, establishment of soft open locations (SOPs), optimum reorganization of networks (ONR), including demand-side (DR) programs. Ensuring the sustainability of electricity networks requires the implementation of these methods [11].

In order to optimize the multiobjective function, the research carried out in [12] used simultaneously planning of interrupters (CBs) and optimum network reconfiguration (ONR). This function included the voltage deviation index, loss a decline, and stochastic distribution production (DG) producing capacity. Switch openings and exchanging (SOE) and achievement history-based adaption development of variations (SHADE) are two techniques used to manage the variability of loading conditions and uncertainties associated with wind turbine (WT) and solar energy (PV) systems (VDI). The research optimized power losses in energy distribution networks using an enhanced variant of the Binary Optimizing particle swarm (BPSO) method, called the Improved BPSO (IBPSO). Problems with setup and capacitor placement were the main focus of the investigation. In this work, a customized evolutionary algorithm (DGA) is presented that concurrently optimizes, under various load situations, how to distribute of fixed or changed interrupters (CBs) in electronic distribution lines (EDNs) and the performance of distributed electricity (DG) units. Many goals are sought after by the function, such as lower operating costs, less system losses, better voltage profiles, and higher voltage stability indices. A technique known as coincident ONR and CB allocation based on personalized optimizations of particle populations (MPSO) was presented in reference [13] to improve power factor, voltage profile, and power losses in order to increase the dependability of the distribution of power system. By assigning ONR and CBs, a modern artificial population optimizing (EABCO) approach was presented in [3, 14] with the goals of minimizing loss, improving the present-day profile, and lowering operational costs. In order to handle the allocation issue of contemporaneous ONR and CBs using the combination of the hybrid broadband-big compression (HBB-BC) technique, a multi-objective mechanism was created in [15]. The function's goals take into account load balance, voltage characteristics, and real

electrical power loss. In ref. [2], the simultaneous ONR and CB allocation problem was successfully resolved with the use of particle swarm optimization (PSO) and randomized frog-leaping algorithms (SFLA). The strategy is to save operating costs while raising reliability and voltage stability directory level. Moreover, reference [16] provides a thorough analysis of many concurrent allocation of ONR and CBs. Nevertheless, in order to properly handle a considerable amount of network unpredictability, the current solutions still need to concentrate coordinated development between these two approaches.

Therefore, instead of concentrating on only one option, the literature evaluation of planning research reveals several advantageous outcomes associated with allocating CBs, the Office of Naval Research, and their combination. To ensure a secure and reliable electrical supply, it is necessary to conduct operational studies that involve simultaneous switching of the Distribution Network Operator (DNO) and Customer's Breaker (CB) while also handling uncertainties related to Active Distribution Networks (ADNs) with Renewable Energy Sources (RESs) and Electric Vehicles (EVs). The investigations have prioritized primary aims such as reducing losses, improving voltage profiles, enhancing stability and reliability, reducing switching costs, and lowering the installation costs of circuit breakers. The majority of research has proprioritized multi-objective functions over single functions. Furthermore, it has been characterized as a complex optimization issue involving multiple variables, which might be either continuous or discrete. Met heuristic techniques are now attracting significant interest in the literature for effectively addressing complex problems. The no-free-lunch argument [5] asserts that not every method is appropriate for solving particular real-time problems related to optimization, and numerous methods encounter premature convergence issues due to insufficient exploration or exploitation capabilities. These gaps motivate researchers to create new metaheuristics or modify existing algorithms. The study's primary contributions are outlined in these aspects and compared to existing literature.

This study significantly advances the field of power grid management by introducing a dynamic, multi-period intelligent traffic allocation algorithm that leverages multi-objective data mining to effectively integrate renewable energy systems (RESs) and electric vehicles (EVs) into the grid. The major contributions include the development and application of the novel Dynamic Optimal Network Reconfiguration (DONR) and Capacitor Bank Switching (CBS) strategies, which together enhance the grid's ability to manage the variability and unpredictability of renewable energy sources and the charging demands of EVs. These strategies help to stabilize the grid by improving voltage profiles, reducing energy losses, and facilitating cost-effective energy distribution throughout the grid's 24-hour operational cycle. Another key contribution is the adaptation and implementation of the Artificial Hummingbird Algorithm (AHA), which is utilized for the first time in this context to solve complex multi-objective optimization problems associated with grid management. The AHA capability to handle multiple, often conflicting objectives - such as minimizing energy loss while maximizing cost efficiency and maintaining grid stability under varying load conditions - represents a significant technological advancement. Furthermore, the extensive testing of this algorithm on an enhanced IEEE 33-bus benchmark system provides empirical evidence of its effectiveness. The simulations conducted compare the AHA performance against traditional algorithms, demonstrating its superior capability in real-time applications. This not only validates the integrated approach of DONR and CBS but also showcases the potential of advanced data mining techniques in optimizing grid operations to meet the challenges posed by high penetrations of RESs and EVs. This comprehensive approach contributes to the broader goals of sustainable development by promoting more efficient and reliable use of energy resources within the power grid.

Following this introductory section, the paper is organized in the following manner: Section 2 theoretically represents the behavior of loads, photovoltaic solar power sources. Section 3 presents a mathematical account of the proposed multipurpose function, together with its operational constraints, both equal and unequal. Section 4 provides a mathematical representation of butterfly foraging and flight and the methodology used to solve it. Section 5 presents outcomes standardized several scenarios. Section 6 provides a concise overview of this study's primary accomplishments and discoveries.

2 MODELING OF THEORETICAL CONCEPTS

The next section provides an explanation of the computational simulations of active transportation system elements, specifically loads, photovoltaic arrays, and shifting banking of capacitors.

2.1 Proposed Composite Load Modeling

Every sub-feeder inside a practical supply chain can cater to a specific customer category. This study investigated the extent to which electric vehicle (EV) charging is integrated into the power grid and all categories of loads associated with EV charging. Within a specific bus system, 90% of the total load is allocated to the genuine network demand, while 10% of the total is classified as the electric vehicle load. The framework considers the monthly variations in both networking consumption and the amount of EV stress, in addition to the expected growth of the EV fleet and its consequences.

$$\bar{P}_{d,h(i)} = 0.9\kappa_{lt,h(i)}P_{d(i)} + \left\{0.1\nu_{h(i)}P_{d(i)}\left(1+\lambda_{ev,g}\right)\right\}, \forall N_{bus} \quad (1)$$

$$\bar{Q}_{d,h(i)} = 0.9\kappa_{lt,h(i)}Q_{d(i)} + \left\{0.1\nu_{h(i)}Q_{d(i)}\left(1+\lambda_{ev,g}\right)\right\}, \forall N_{bus} \quad (2)$$

wherein $\kappa_{lt,h(i)}$ and $\nu_{h(i)}$ denote the hourly fluctuations of a particular load type at bus-*i*, with EV load, accordingly; $\lambda_{ev,g}$ represents the percentage increase in EV load; $P_{d(i)}$ and $Q_{d(i)}$ are the statutory accurate as well as categorization of battery reactive loads at bus-i, correspondingly; The annual real and reactive electrical loadings that include the EV load are represented respectively. *N* is the number of vehicles overall in the system.

2.2 Modeling of Photovoltaic Systems

With a solar energy system (PV that connects Roofing rooftops or balconies are connected to the electricity grid by a power converter equipment. They may now operate in tandem with the microwave electricity network thanks to this. Through the use of an inverter, which optimizes the gathering of direct-current (DC) electricity generated by the solar panel array, exceptional AC electricity is produced and easily connected to the electricity grid. As a result, the converter may generate the optimal quantity of alternating current (AC) electricity. We can integrate a PV system to calculate the net functional real power that is responsive loads on bus I.

$$\bar{P}_{d,h(i)} = \bar{P}_{d,h(i)} - P_{pv,h(i)} \tag{3}$$

$$\bar{Q}_{d,h(i)} = \bar{Q}_{d,h(i)} - P_{pv,h(i)} \tan\left(\cos^{-1}\varphi_{i(h)}\right) \tag{4}$$

The climate where a system for photovoltaic is installed affects how much electricity it can produce. To estimate the weekly fluctuation of power generation, factors such as radiance and temperature are taken into account [17]. The following equation expresses this:

$$P_{pv,h(i)} = S_{pv(i)}\eta_{stc} \left\{1-\beta_{tem}\left[\left(T_{amb}+\frac{(NOCT-20)G_{(h)}}{800}\right)-T_{stc}\right]\right\} \tag{5}$$

where $P_{pv,h(i)}$ is the actual power administration by solar energy systems into the electrical supply via the transformer, $S_{pv(i)}$ is the electrical power measure at which the PV inverters operate, $C(h)$ is the installed capacity of the PV system, η is the effectiveness of the solar panels at the typical test environment (STC), α is the Celsius value, β_{tem} is the substrate the climate. The optimum and conventional temps of operation, as specified according to the maker, are T_{amb} whereas T_{stc} at Syracuse Technical College, whereas the weekly amount of sunlight at the PV place of residence.

2.3 Modeling of Switched Capacitor Banks

Changed banked capacitors (small and medium-sized) are intended to be turned off as well as on based on the energy component at specific times reactivity, and polarity. Fluctuations in the amount of work result in a specific quantity of changeover actions occurring daily. Changing the method of connecting and disconnecting reactive demand from the electricity grid may occur multiple times a day to ensure the proper voltage levels of the system are maintained. The VAr administrations by SCBs are mimicked by using granular step-level regulation.

$$\bar{Q}_{d,h(i)} = Q_{d,h(i)} - \gamma_{h(i)}Q_{cb(i)} \tag{6}$$

where $\gamma_{h(i)}$ denotes the independent step adjustment level of the Static Circuit Breaker (SCB) at bus-*i*, and $Q_{cb(i)}$ indicates the most significant potential of the SCB at bus-*i*.

2.4 Problem Formulation

The following part describes the graphical representation of the suggested multipurpose variable and its corresponding equivalent and uneven restrictions at the administrative level.

2.5 Objective Function

A multiple-purpose functionality is created to minimize shipping damages, enhance voltage characteristics, decrease operating expenditures, and maximize total savings.

$$OF = \min\left\{\frac{1}{T}\left[\sum_{h=1}^{T}\left(P_{loss(h)} + AVD_{(h)} + C_{s(h)}\right)\right]\right\} \tag{7}$$

where $P_{loss(h)}$, $AVD_{(h)}$, $C_{s(h)}$ or h represent the monthly distributions of actual Solutions (8) to (10) specify loss of electricity, average amplitude fluctuations, then overall money, respectively; T represents the value entirety of the period spent in simulation.

$$P_{loss} = \sum_{br=1}^{N_{br}}\left\{\left(\frac{V_{(i)}-V_{(j)}}{Z_{br(ij)}}\right)^2 r_{br}\right\} \tag{8}$$

$$AVD = \frac{1}{N_{bus}}\left\{\sum_{b=1}^{N_{bus}}\sqrt{\left(\frac{V_{(s)}-V_{(i)}}{V_{(s)}}\right)^2}\right\} \tag{9}$$

$$C_s = \tau_{loss}P_{loss} - \left(\tau_{cb}Q_{cb,T} + \tau_{sw,c}n_{sw,c} + \tau_{sw,b}n_{sw,b}\right) \tag{10}$$

where $V_{(i)}$ is the electricity corresponding to bus- $Z_{br(ij)}$ is the branching obstruction across coaches *I* as well as *J*, each branch blockages $Q_{cb,T}$ the overall amount of affiliated companies within the distribution system N_{bus}, and the costs associated with actual electric power loss, VAr administration for small and medium-sized, the conversion cost of small and medium-sized, and the becoming expense of additionally sectionalize nor tie-line, respectively, are represented by the numbers (A1), (A2), (A3), (A4), as well as (A5). All small and medium-sized throughout the system promote the entire VAr (Q1) (Q2) and (Q3) is the quantity of changing operations of SCBs and a combination of sectionalized or tie-line, accordingly.

2.6 Operational Constraints

The PV integrator power factor: The PV inverter's operational power factor is critical in maintaining a

suitable voltage strength at the optimum level of shared coupling, or PCC (point of common coupling), by providing the required VAr support. This job is limited within the spectrum that came before it in every operating period since operating inverters that convert solar energy at a deficient voltage factor might reduce the amount of actual power pumped into the grid.

$$0.85 \le \cos\varphi_{i(h)} \le 1.0 \text{ and } \forall h \tag{11}$$

Var limit: To avoid exaggeration and consequent overvoltage, the volume of reactive power injection from the inverters for solar energy or CBs should not exceed the total reactionary power demand of the network. For each working hour, the following constraint is taken into account in this study:

$$\left(\sum_{i=1}^{N_{cb}} \gamma_{h(i)} Q_{cb(i)} + \sum_{j=1}^{N_{pv}} Q_{pv,h(i)}\right) \le \sum_{k=1}^{N_{bus}} \bar{Q}_{d,h(k)} \forall N_{pv} \text{ and } \forall h \tag{12}$$

Bus voltage value limit: To prevent reverse electrical energy from a connection to the grid, bus electrical voltage dimensions should always be less than or as near to the lowest possible bus voltage significance as feasible. Furthermore, bus voltage dimensions are designed to function within predefined boundaries to avoid issues with low or excessive voltage.

$$V_{h(i)} \le V_{(s)} \forall h_{bus} \tag{13}$$

$$V_{\min} \le V_{h(i)} \le V_{\max} \forall N_{bus} \tag{14}$$

Rituality restriction: Preventative mechanisms are designed for an identified electrical flow orientation from headwaters to downstream since most EDNs have radial configurations. As a result, even when changing the network architecture, it is essential to maintain the radiality constraint. To guarantee this, the following requirements must always be satisfied.

$$N_{br} + N_{tie} = N_{bus} - 1 \forall h \tag{15}$$

wherein N_{tie} is the working coefficient of $V_{\min}$ and $V_{\max}$ converters; $\cos\varphi_{i(h)}$ correspondingly, the minimal or greatest amounts on the buses include maximum or maximal current dimensions.

3 MODELING OF MIGRATION FORAGING

The Honeysuckle travels to a distance-feeding place when the food supply runs low at its regular eating location. The AHA defined the migrating coefficient. Humming birds move to a generated at random food supply throughout the search area if the total number of repetitions surpasses the movement frequency.

After that, the insect in question switches to the new source and stops using the old one, updating the visit table. Here is a description of a humming bird's migration as it forages from one honey resource to another.

$$x_w(t+1) = l + r \times (u - l) \tag{24}$$

where the primary nourishment supply is in those individuals with the lowest rate of nectar replenishment. The relationship between the overall population count and the movement of people coefficient is $m = 2n$. Fig. 1 shows a flow chart that illustrates every step in utilizing AHA to solve the suggested improvement algorithm. Refer to [18] for a more thorough discussion of each step involved in implementing AHA.

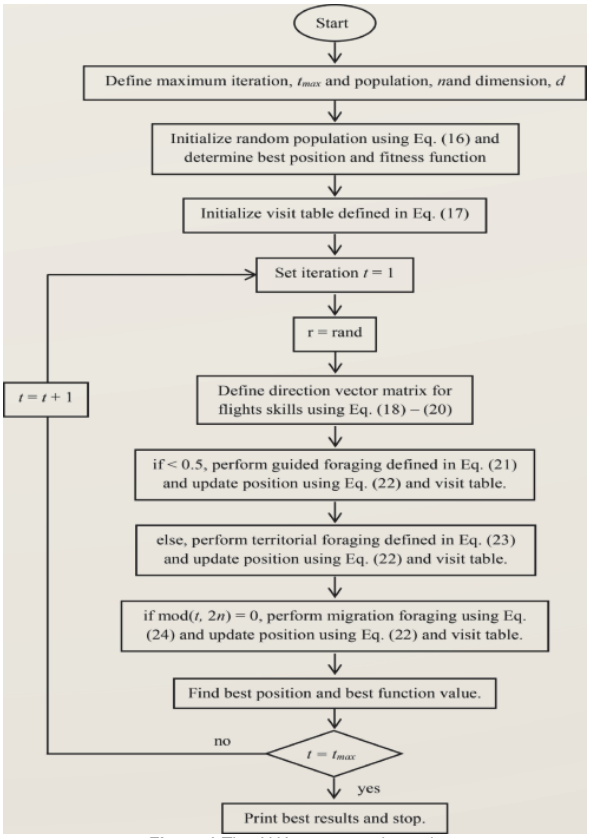

Figure 1 The AHA process schematic

4 RESULTS AND DISCUSSION

Enhancements to the IEEE 33-bus standard evaluation apparatus were used to evaluate the efficacy of the suggested technique [19]. Four 0.2 MW DG units are located at busses 18, twenty-two, 25, and 33 in the test system. Furthermore, reactive electricity with sensitivity is also installed on buses 18 and 33. By comparison, it has two tie lines that link buses 8-21, 12-22 and 25-29, in that order. It was believed that sectionalized exchanges were present in all 32 network segments. Fig. 2 displays an illustration of the test apparatus under such presumptions.

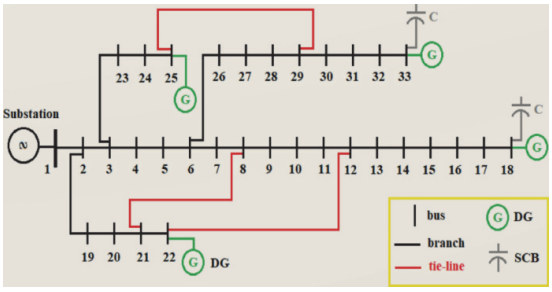

Figure 2 Expanded IEEE 33-bus test apparatus arrangement

Furthermore, regarding the circumstances of the network's fluctuation, the subsequent assumptions were developed: as demonstrated in Fig. 3, the average daily load distribution is produced by normalization to the day's highest demand [20]. Each of the four DGs was handled as a PV-typeDG. Using the Watts Calculator developed, the electricity production levels were determined based on production. By standardizing to its peak production, the monthly solar power production curve is produced from this data, as shown in Fig. 4. Moreover, as seen in Fig. 5, the EV recharge demand curve is anticipated.

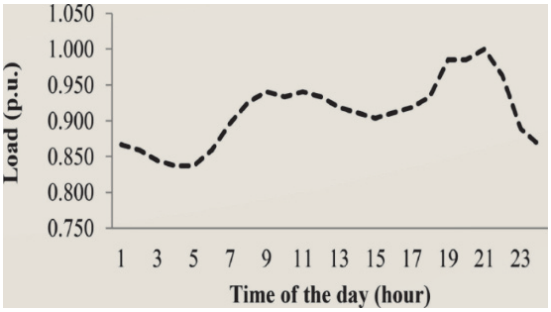

Figure 3 An average weekly capacity curve adjusted to the morning's highest load

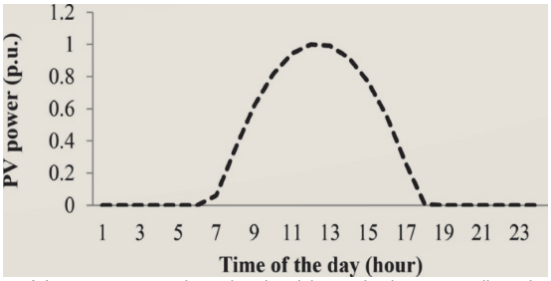

Figure 4 An average everyday solar electricity production curve adjusted to the morning's peak production

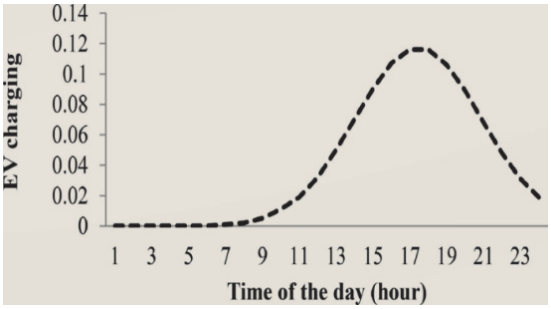

Figure 5 Requirement pattern for charging for electric vehicles

In these conditions, network-level volt/VAr controls are built by optimizing the VAr generated by CBs at busses 18 and 33, and a total of three tie-lines and 32 sectionalizes are turned on and off to adjust the network's topology. As a result, the area to be searched in the optimization query is transformed into discrete variables for shutting or extending any three sectors from triple tie wires and 32 sectionalizes, and a constant parameter for the VAr results from CBs based on their ratings.

Tab. 1 lists the EV sales over the last five decades, per 33. The rate of increase for each successive year was estimated in 2017, and the EV load multiplier was calculated as a result. 10% of each bus's basic load was considered the network's basic EV load. The modeling procedures are carried out in accordance with Tab. 1's projection for 2021, which states that the EV penetration factors 2.815 in the direction of a substantial share of the demand for EVs.

Table 1 Sales projections for EV loads in the Indian state of Andhra Pradesh

Vehicle Type	2017	2018	2019	2020	2021	2022
Motorcycles	3100	3285	4710	5920	8150	15,200
Rickshaws	105	10	120	695	160	2600
Cars	2500	3550	4100	4150	4250	4600
Total	5705	6845	8930	10,765	12,560	22,400
Growth Rate	-	0.199	0.524	0.818	1.167	2.07

The selected costs are 168 $/kilowatt, 0.65 $/kVAr, 1 $/changing, and 2 $/switching for the expenses of loss τ_{loss}, cost of responsive electrical supply via CBs τ_{cb} cost of Cbr changing $\tau_{sw,c}$, and cost of branches switching $n_{sw,b}$. The minimum and lowest total number of repetitions for each case study were determined to be thirty and fifty, respectively. The next trio of scenarios underwent extensive simulation and comparison.

Case 1: Volt/var control considering only switching of CBs

In this case, it was taken for granted that the network had a radial structure by neglecting tie lines. Therefore, controlling the VAr production through CBs is the only option to reduce the impact of unpredictability on the network. Tab. 2 displays the actual and reactive electricity expenses, deviation from the voltage index, changing states, and corresponding net savings for both regulated and unregulated systems with optimal values of CBs without AHA for each hour.

Table 2 The functioning of the network in Case 1 between the two-combination volt-van controls

Hr	Before volt/VAr Controls	After volt/VAr Controls	VAr Injections	$n\_(sw, c)$	C_s
	$P\_(\text{loss}(h))$	$Q\_(\text{loss}(h))$	$AVD\_((h))$	$P\_(\text{loss}(h))$	$Q\_(\text{loss}(h))$
1	125.48	85.2	0.0025	91.59	63.93
2	122.56	83.15	0.0024	89.82	62.73
3	118.11	80.33	0.0023	86.54	60.5
4	116.06	78.94	0.0023	85.04	59.49
5	116.06	78.94	0.0023	85.04	59.49
6	122.56	83.15	0.0024	89.82	62.73
7	130.81	88.86	0.0026	95.19	66.3
8	125.4	84.86	0.0025	87.93	61.05
9	117.66	79.43	0.0023	79.4	55.09
10	107.73	72.66	0.0021	70.28	48.88
11	105.75	71.32	0.002	67.6	47.06
12	102.95	69.44	0.0019	65.1	45.39
13	101.6	68.53	0.0019	64.24	44.8
14	104.56	70.52	0.002	67.04	46.68
15	110.86	74.78	0.0021	72.97	50.69
16	124.61	84.15	0.0024	85.12	59.01
17	143.02	96.87	0.0028	101.87	70.6
18	162.33	110.31	0.0032	119.28	82.75
19	180.11	122.39	0.0035	132.74	91.94
20	177.43	120.57	0.0035	130.71	90.55
21	179.7	122.11	0.0035	132.42	91.71
22	163.17	110.89	0.0032	120	83.27
23	135.9	92.4	0.0027	99.67	69.42
24	127.43	86.65	0.0025	93.41	65.17

The median actual and reactive electricity outputs are lower when compared to the effectiveness of the non-compensation equipment; bus 18 and 33 need VAr settings of 297.29 kivas and 600 VAr, respectively. Since the

lowest step change is five kivas, 36 switching procedures are in total. The net reductions as a whole averaged 5774.83 $/h.

Case 2: Volt/var control considering only reconfiguration

In this instance, it is assumed that there are no CBs in the telecommunications system, only tie lines. Therefore, the goal is to increase network performance with minimal topological modifications. Tab. 3 lists the outcomes of the Hop for every single hour. The network performance is demonstrated regarding reactive and actual power losses, deviations in voltage index, changing states, and related net savings for each working day with the primary case setup and optimum reconfirming achieved AHA.

Table 3 The operation of the wireless network in the second scenario with and without mixed voltage management

Hr	Before volt/VAr Controls	After volt/VAr Controls	VAr Injections	$n\_(sw, b)$	C_s
	$P\_(\text{loss}(h))$	$Q\_(\text{loss}(h))$	$AVD\_((\text{h}))$	$P\_(\text{loss}(h))$	$Q\_(\text{loss}(h))$
1	124.98	84.99	0.0023	86.93	65.07
2	122.56	83.35	0.0022	85.29	63.85
3	118.11	80.33	0.0021	82.26	61.59
4	116.06	78.94	0.0021	82.25	59.61
5	116.06	78.94	0.0021	80.87	60.55
6	122.56	83.35	0.0022	85.29	63.85
7	130.81	88.86	0.0024	90.46	67.52
8	125.4	84.86	0.0023	85.02	62.69
9	117.66	79.43	0.0021	78.51	57.3
10	107.73	72.66	0.0019	71.18	51.61
11	105.75	71.32	0.0018	69.47	50.2
12	102.95	69.44	0.0017	67.49	48.7
13	101.6	68.53	0.0017	66.86	48.43
14	104.56	70.52	0.0018	68.78	49.73
15	110.86	74.78	0.0019	73.4	53.3
16	124.61	84.15	0.0022	83.42	61.05
17	143.02	96.87	0.0026	97.33	72.04
18	162.33	110.31	0.003	112.08	83.8
19	180.11	122.39	0.0033	126.18	91.31
20	177.43	120.57	0.0033	122.26	91.42
21	179.7	122.11	0.0033	123.78	92.55
22	163.17	110.89	0.003	112.7	84.29
23	135.9	92.4	0.0025	94.33	70.59
24	127.43	86.65	0.0023	88.6	66.31

When compared the median real and reactivity losses of electricity dropped from (129.06 kW + j87.19 kVAr) because of the non-compensation mechanism functioning other hand, 20 switching operations were required to alter the system's topology. The average total savings per hour waswere03.03 $/hour.

Case 3: Volt/var control considering both CBs and reconfiguration

In this situation, combiningCBs and network settings is preferableto achieve volt/VAr regulation through the network. The simulations were run accordingto the changes results are given below. The network's efficiency for each hour is shown in Tab. 4 losses are expressed in kW and ovary, respectively. The AVD was supplied in pun. The reactive power infusions generated presented in VAr, while the net savings are displayed in USD. These volt/VAr modifications reduce the average loss of power byabout(129.06 kW + j87.19 kVAr) down (63.65 kW + j47.44 kVAr), respectively. Because of the almost zero average voltage variance, the network canmaintain an adequate voltage profile at all sites throughout the day. CBs inject electrical power at sites 18 and 33, averaging 211.67 kivas or 600 kVAr, respectively. Because bus 33's CB value doesn't change throughout the day, only bus 18 is impacted by the CB changeover cost. For CBs and topology modifications, there were 27 and 38 switching operations, respectively. 10,457.12 $/h was computed as the median total reduction in operating expenses for the whole day.

Table 4 The efficiency of the network in Case 3, both with and without combining volt/VAr management

Hr	$P\_\text{loss}(h)$	$Q\_\text{loss}(h)$	$AVD(h)$	$P\_\text{loss}(h)$	$Q\_\text{loss}(h)$	$AVD(h)$	$Q\_cb(18)$	$Q\_cb(33)$	n_sw, b	n_sw, c	C_s
1	125	85	0.0025	64	48.5	0.0005	200	610	0	0	9650
2	122.5	83.5	0.0024	63	47.5	0.0005	200	610	0	0	9450
3	118	80	0.0023	60.5	46	0.0005	195	610	0	1	9080
4	116	78.5	0.0023	63	47	0.0005	195	610	4	0	8300
5	116	78.5	0.0023	59.5	45	0.0005	195	610	4	0	8905
6	122.5	83.5	0.0024	63	47.5	0.0005	200	610	0	1	9450
7	130.5	88.5	0.0026	66	50	0.0005	210	610	0	2	10,240
8	125	84.5	0.0025	60.5	45	0.0005	215	610	0	1	10,315
9	117.5	79	0.0023	54	39.5	0.0004	225	610	2	2	10,090
10	107.5	72	0.0021	47	34.5	0.0004	220	610	0	1	9530
11	105.5	70.5	0.002	44.5	33	0.0004	225	610	2	1	9595
12	102.5	68.5	0.0019	42.5	31.5	0.0003	225	610	0	0	9440
13	101	67.5	0.0019	44.5	32	0.0003	215	610	4	2	8905
14	104	69.5	0.002	44	33	0.0003	220	610	4	1	9450
15	110.5	74	0.0021	49	36.5	0.0004	225	610	0	1	9755
16	124	83.5	0.0024	57.5	42.5	0.0005	225	610	2	0	10,575
17	143	96.5	0.0028	73.5	54	0.0005	215	610	6	2	11,050
18	162	110	0.0032	83	62.5	0.0007	230	610	6	3	12,685
19	180	122	0.0035	92.5	69	0.0008	240	610	0	2	14,120
20	177.5	120	0.0035	91	68	0.0008	240	610	0	0	13,905
21	179.5	121.5	0.0035	92	69	0.0008	240	610	0	0	14,085
22	163	110.5	0.0032	83.5	62.5	0.0007	230	610	0	2	12,755
23	135.5	92	0.0027	69.5	52.5	0.0006	210	610	0	4	10,540
24	127	86	0.0025	69	51.5	0.0006	205	610	4		

Tab. 5 compares the network structure modifications for Instances 2 and 3. However, the typical total savings in Case 3 are higher than in Case 1.

Table 5 The hourly best network architecture for Cases 2 and 3

Case 2		Case 3	
Time of the day (hr)	Open switches	Time of the day (hr)	Open switches
1 to 2, 4 to 11, 13 to 17, 19 to 23	6, 12, 29	1 to 2, 4 to 7, 17 to 22	6, 12, 36
3, 18	9, 29, 34	3, 21	9, 34, 36
12	6, 8, 29	8	8, 9, 17
			8, 12, 29
	6, 12, 29	13	7, 29, 34
	16	16	7, 9, 34

Fig. 6 to Fig. 8 compare the actual blackouts, loss of reactionary electricity, and variations in the network's average voltage drop under various circumstances. The comparison shows that the original network did not include volt/VAr controls and had a low voltage profile, significant distribution losses, and loss. The parameters above are improved more significantly when CB control and ONR are combined, but they are improved more significantly when CB control and ONR are used separately. Fig. 9 illustrates the cost reduction compared to the uncompensated condition. Compared to stand-alone techniques the combined strategy results in considerable savings due to its significant reduction in power losses. On the other hand, the ONR outperformed the CB oversight in every way. Consequently, to tackle uncertainties, installation in addition to CBs.

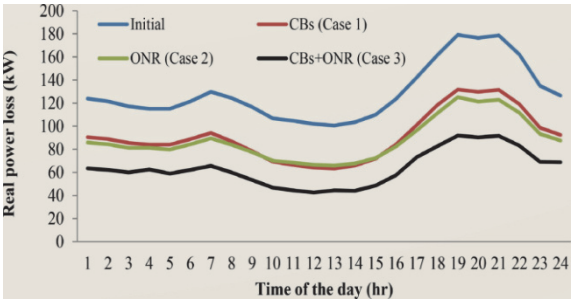

Figure 6 Real losses in power comparisons for various conditions

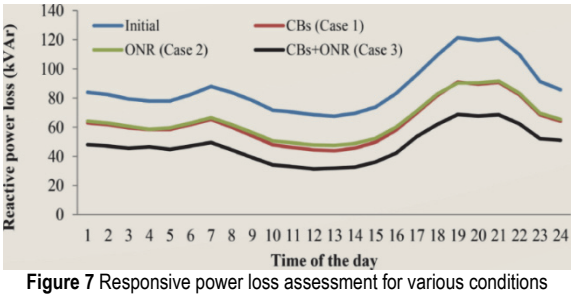

Figure 7 Responsive power loss assessment for various conditions

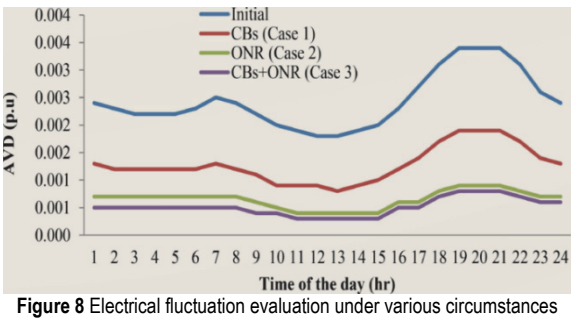

Figure 8 Electrical fluctuation evaluation under various circumstances

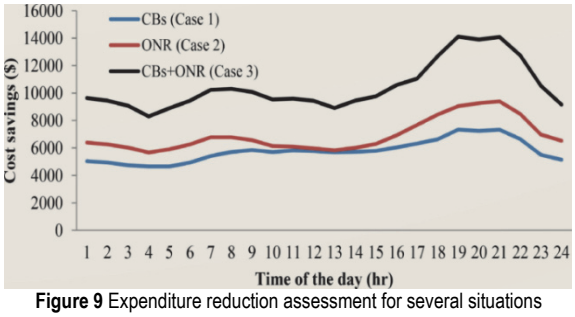

Figure 9 Expenditure reduction assessment for several situations

5 COMPARATIVE ANALYSIS

5.1 Dynamic optimal volt/VAr controls

Other modern artificial intelligence, such as optimization technique coati optimization technique (COA), and cheetah optimization, are compared with the outcomes of AHA. Under access to data, you can get the specifics of the mathematical code for these methods, which includes the AHA. Tab. 6 lists the median actual power loss that each method produced.

Table 6 Comparison of several methods by averaged Plods

Algorithm	Average P loss / kW		
	Case 1	Case 2	Case 3
(Doe & Smith, 2024)	88.5	86	63.5
(Johnson et al., 2020)	90.25	87.95	62
(Lee & Kumar, 2021)	92.1	85.5	64
(Brown & Garcia, 2020)	88.5	86	63.5
(Martinez & Wong, 2021)	90.25	86.75	64

In Case 1, the documentation of possession has the biggest power loss, the GOA as well as PD have the smallest losses, and the POA has second-greatest energy loss compared to the AHA. The POA lost its greatest amount of power in Case Two, with the AHA coming in second, the Public Power Transmission Organizations (PPTO) and GOA coming in third, and the COA coming in last. The POA suffers the smallest power outage in Case 3, with the COA and AHA tying for the second-lowest loss of energy and the PPTO and GOA sharing the third-lowest loss of power.

We evaluated the average performance of all the algorithms and sorted them based on how well they performed in each of the three circumstances (examples 1, 2, and 3). POA saw the least significant average reduction in power of the three scenarios. COA displayed the second-lowest aggregate loss of energy of all the cases. With a little higher average power loss than POA and COA, AHA comes in third place. In contrast, the PPTO as well as GOA are equal for fourth position in the critical typical loss in electricity values between each of the possibilities standings. This research increases the search variety and exploratory capacity. Fundamental AHA has to improve substantially.

5.2 Optimal Var Controls

This section compares the computing power of AHA with well-known computer programs, including PSO, instruction using statistical measurements based on 50 separate testing sessions for each example. Additionally, Tabs. 7, 8, and 9 provide the AHA's findings for CB reservation, ONR, and concurrent CB allocation in

comparison to literature studies. Using normal IEEE 33-bus data, calculations were run into account.

Table 7 Cbr cooperation at its best

Method	CB Sizes in MVAr (bus #)	P_loss / kW	V_min in p.u. (bus #)
Base	-	201.75	0.9120 (18)
EGA-PSO (Baker et al., 2017)	0.4200 (13), 0.5600 (24), 1.1400 (30)	131.2	0.9360 (18)
HBA (Wang et al., 2022)	320 (6), 295 (13), 710 (29)	134.1	0.9350 (18)
PSO	1.000 (30), 0.3600 (13), 0.8800 (3)	132.3	0.9460 (18)
TLO	0.3800 (13), 0.4300 (25), 1.0400 (30)	131.4	0.9360 (18)
CSA	0.4300 (12), 0.5300 (24), 1.0100 (30)	131.2	0.9350 (18)
AHA	0.3700 (13), 0.5400 (24), 1.0300 (30)	131.2	0.9360 (18)

Table 8 Reconfiguring the system optimally

Method	Open switches	P_loss / kW	V_min in p.u. (bus #)
Base	33, 34, 35, 36, 37	201.75	0.9120 (18)
Reference results	8, 10, 15, 31, 38	138.5	0.9350 (18)
HGA (Smith & Lee, 2024)	8, 10, 15, 31, 38	138.5	0.9350 (18)
PSO	8, 10, 15, 31, 38	138.5	0.9350 (18)
TLA	8, 10, 15, 31, 38	138.5	0.9350 (18)
COA	8, 10, 15, 31, 38	138.5	0.9350 (18)
ACO	8, 10, 15, 31, 38	138.5	0.9350 (18)

Table 9 Concurrent changes to the network and CB assignment

Method	CB Sizes in MVAr (bus #)	Open switches	P_loss / kW	V_min in p.u. (bus #)
Base	–	33, 34, 35, 36, 37	201.75	0.9120 (18)
EGWO-PSO (Baker et al., 2023)	0.210 (28), 0.230 (29), 0.560 (30)	8, 10, 15, 31, 38	100.75	0.9530 (32)
PSO	1.000 (30), 0.610 (21), 0.800 (2)	8, 10, 15, 31, 38	95.55	0.9550 (33)
TLO	0.320 (12), 0.180 (33), 1.020 (30)	8, 10, 15, 31, 38	94.27	0.9620 (32)
CSA	0.390 (12), 0.640 (23), 0.950 (30)	8, 10, 15, 31, 38	93.93	0.9530 (33)
AHA	0.530 (24), 0.310 (15), 0.960 (30)	8, 10, 15, 31, 38	93.28	0.9610 (33)

5.2.1 Assignment of Capacitors

The actual and reactivity power demands of the IEEE 33-bus standard test system are 3715 or 2300 cars, respectively. The system's base case performance was as follows. Reactive energy losses were 135.141 kVAr, and actual electricity losses were 202.6771 kW. At bus-18, the lowest voltage measured was 0.913 p.u. In this case study, the system's performance was enhanced by optimally integrating CBs; the outcomes are detailed in Tab. 7. The outcomes of the polar bear optimizing method are all inferior to the suggested AHA, 38. At busses 13, 24, and 30, the ideal is 1.0372, in that order. The lowest voltage strength 18 is increased to 0.938 p.u. The system's genuine losses are decreased to 132.17 kW.

5.2.2 Reconfiguring the Internet Connection

Five tie connections in the IEEE 33-bus standard may be used to change the network setup. As demonstrated in Case A, the base instance throughput is still the same. Tab. 8 presents a comparison between the optimum configuration achieved by the AHA and the benchmark results found in references [21], are the best choices for enhancing network performance. The minimal voltage amplitude at bus-18 was increased to 0.9362 p.u., and the network losses decreased to 139.551 kW. The AHA findings are comparable to every analyzed trial and show outstanding concurrence overall with the previous year's results.

5.2.3 Distributing CBs in the Best Possible Network Design

Three CBs were ideally distributed to the modified network, which was the best option in Case B. The outcomes are shown in Tab. 9. Switches 7, 9, 14, 32, and 37 are the best choices for enhancing network performance. At busses 24, 15, and 30, the AHA determined that the best CBs in MVAr comprised 0.5285, 0.3132, and 0.9648, respectively. The network's actual loss values were decreased to 93.278 kW. Compared to other techniques like the changed pollination of technique (MFPA), the AHA yields better outcomes.

6 CONCLUSION

This study underscores the successful development and implementation of a dynamic, multi-period intelligent traffic allocation algorithm designed to optimize the integration of renewable energy systems (RESs) and electric vehicles (EVs) into power grids. The findings from the research demonstrate that by employing a combination of Dynamic Optimal Network Reconfiguration (DONR) and Capacitor Bank Switching (CBS), the power grid can effectively manage the inherent variability and unpredictability of renewable energy and EV load demands. This integrated approach not only stabilizes the grid but also enhances operational efficiencies, reducing energy loss and improving voltage profiles across a continuous 24-hour cycle.

A key component of this research was the application of the Artificial Hummingbird Algorithm (AHA), a novel method adapted specifically for this study to tackle complex multi-objective optimization problems. The AHA proved particularly adept at navigating the challenges posed by fluctuating solar power outputs and the diverse load requirements introduced by high penetrations of electric vehicles. The rigorous testing on the enhanced IEEE 33-bus benchmark system offered a robust platform for evaluating the algorithm's computational effectiveness and comparing its performance against existing algorithms. These tests confirmed that the AHA outperforms traditional optimization methods in real-time scenarios, offering a more effective solution for dynamic grid management. Cooperation between the Office of Nuclear Regulation and CBS provides significant advantages, such as less energy loss, enhanced voltage stability, and cost optimization during round-the-clock operations, especially regarding increased electrical vehicle (EV) demand

integrating. Using an improved with the institute's 33-bus standardization system, the AHA's calculating process may be thoroughly examined in comparison to other algorithms of a similar kind. In the beginning point scenario, network differences lead to average losses of 87.19 kVAr and reactive power (129.06 kW). In Case 1, monthly losses reduce of resulting in net savings of 5774.83 $/h. However, Case 2 shows that a simple dynamic reconfiguration may boost the overall savings to 6903.03 $/h and decrease in efficiencies at (87.95 kW + j64.72 kVAr). Furthermore, by combining VAr control with effective reconfiguration, losses may be reduced (63.65 kW + j 47.44 kVAr), yielding a noteworthy financial savings of 10,457.12 $/h. The improved efficacy of combining DONR& CBS for purposes is shown by this research that operate in real-time, outperforming other approaches in distributed network reliability optimization.

The study's approach not only contributes to the technical fields of electrical engineering and energy management but also aligns with global sustainability goals. By improving the efficiency and reliability of power grid operations through advanced data mining and optimization techniques, the study supports the broader objective of reducing environmental impact and promoting sustainable energy practices. The successful implementation of the DONR and CBS strategies, coupled with the AHA, illustrates the potential for such innovative methodologies to transform grid management practices, making them more adaptive to the evolving energy landscape marked by increased reliance on renewable energy sources and electric vehicles.

This research paves the way for future investigations into the scalability of these techniques and their applicability to other complex systems, potentially leading to widespread adoption and further enhancements in grid management and sustainability efforts worldwide.

Acknowledgement

First and foremost, I would like to show my deepest gratitude to Dr. Guo, who has helped me with valuable guidance in every stage of the thesis. I shall extend my thanks to Mrs. Liu for all her kindness and help. I would also like to thank Silesian College of Intelligent Science and Engineering, Yanshan University, which have helped me to develop the fundamental and essential academic competence.

7 REFERENCES

[1] Lias, K., Basri, H. M., Buswig, Y. M. Y., Jamali, A., Kamaruddin, A. M. N. A., Wong, V. L., Rosli, M. Z. F., & Sahari, S. K. (2024). Development of 9kWp solar system to enhance smoked shrimp (sesarunjur) production at Igan, Sarawak, Malaysia. *E-Prime - Advances in Electrical Engineering, Electronics and Energy*, *7*. https://doi.org/10.1016/j.prime.2024.100459

[2] Jayanthi, S., Raja, P., Elangovan, M., & Murugesh, T. S. (2024). Single ended 12T cntfetsram cell with high stability for low power smart device applications. *E-Prime - Advances in Electrical Engineering, Electronics and Energy*, *7*. https://doi.org/10.1016/j.prime.2024.100479

[3] Hussein, M. A. & Karam, E. H. (2024). Design immune robust integral signum of the error controller for cancer tumor growth treatment based on improved crow search algorithm. *E-Prime - Advances in Electrical Engineering, Electronics and Energy*, *7*. https://doi.org/10.1016/j.prime.2024.100472

[4] Bhatia, K. & Sarode, G. (2024). Exploration of sustainability of micro grid grounding design in proximity to the pole grounding through experimental measurement of safety parameters. *E-Prime - Advances in Electrical Engineering, Electronics and Energy*, *7*. https://doi.org/10.1016/j.prime.2023.100393

[5] Dubey, S., Sarvaiya, J. N., & Seshadri, B. (2013). Temperature dependent photovoltaic (PV) efficiency and its effect on PV production in the world - A review. *Energy Procedia*, *33*, 311-321. https://doi.org/10.1016/j.egypro.2013.05.072

[6] Fu, Y. Y. & Chiang, H. D. (2018). Toward optimal multiperiod network reconfiguration for increasing the hosting capacity of distribution networks. *IEEE Transactions on Power Delivery*, *33*(5), 2294-2304. https://doi.org/10.1109/TPWRD.2018.2801332

[7] Sedighizadeh, M. & Bakhtiary, R. (2016). Optimal multi-objective reconfiguration and capacitor placement of distribution systems with the Hybrid Big Bang-Big Crunch algorithm in the fuzzy framework. *Ain Shams Engineering Journal*, *7*(1), 113-129. https://doi.org/10.1016/j.asej.2015.11.018

[8] Gutiérrez-Alcaraz, G. & Tovar-Hernández, J. H. (2017). Two-stage heuristic methodology for optimal reconfiguration and Volt/VAr control in the operation of electrical distribution systems. *IET Generation, Transmission and Distribution*, *11*(16), 3946-3954. https://doi.org/10.1049/IET-GTD.2016.1870

[9] Mishra, S., Das, D., & Paul, S. (2017). A comprehensive review on power distribution network reconfiguration. *Energy Systems*, *8*(2), 227-284. https://doi.org/10.1007/S12667-016-0195-7

[10] Pandraju, T. K. S. & Janamala, V. (2021). Dynamic optimal network reconfiguration under photovoltaic generation and electric vehicle fleet load variability using self-adaptive butterfly optimization algorithm. *International Journal of Emerging Electric Power Systems*, *22*(4), 423-437. https://doi.org/10.1515/IJEEPS-2021-0009

[11] Lotfi, H., Ghazi, R., & Naghibi-Sistani, M. B. (2020). Multi-objective dynamic distribution feeder reconfiguration along with capacitor allocation using a new hybrid evolutionary algorithm. *Energy Systems*, *11*(3), 779-809. https://doi.org/10.1007/S12667-019-00333-3

[12] Habib, S., Khan, M. M., Abbas, F., Sang, L., Shahid, M. U., & Tang, H. (2018). A Comprehensive Study of Implemented International Standards, Technical Challenges, Impacts and Prospects for Electric Vehicles. *IEEE Access*, *6*, 13866-13890. https://doi.org/10.1109/ACCESS.2018.2812303

[13] Impram, S., VarbakNese, S., & Oral, B. (2020). Challenges of renewable energy penetration on power system flexibility: A survey. *Energy Strategy Reviews*, *31*. https://doi.org/10.1016/j.esr.2020.100539

[14] Saddique, M. W., Haroon, S. S., Amin, S., Bhatti, A. R., Sajjad, I. A., & Liaqat, R. (2021). Optimal Placement and Sizing of Shunt Capacitors in Radial Distribution System Using Polar Bear Optimization Algorithm. *Arabian Journal for Science and Engineering*, *46*(2), 873-899. https://doi.org/10.1007/S13369-020-04747-5

[15] Badran, O., Mekhilef, S., Mokhlis, H., & Dahalan, W. (2017). Optimal reconfiguration of distribution system connected with distributed generations: A review of different methodologies. *Renewable and Sustainable Energy Reviews*, *73*, 854-867. https://doi.org/10.1016/j.rser.2017.02.010

[16] Ismail, B., Abdul Wahab, N. I., Othman, M. L., Radzi, M. A. M., Naidu Vijyakumar, K., & Mat Naain, M. N. (2020). A Comprehensive Review on Optimal Location and Sizing of

Reactive Power Compensation Using Hybrid-Based Approaches for Power Loss Reduction, Voltage Stability Improvement, Voltage Profile Enhancement and Load ability Enhancement. *IEEE Access*, *8*, 222733-222765. https://doi.org/10.1109/ACCESS.2020.3043297

[17] Namachivayam, G., Sankaralingam, C., Perumal, S. K., & Devanathan, S. T. (2016). Reconfiguration and Capacitor Placement of Radial Distribution Systems by Modified Flower Pollination Algorithm. *Electric Power Components and Systems*, *44*(13), 1492-1502. https://doi.org/10.1080/15325008.2016.1172281

[18] Dehghani, M., Montazeri, Z., Trojovská, E., &Trojovský, P. (2023). Coati Optimization Algorithm: A new bio-inspired metaheuristic algorithm for solving optimization problems. *Knowledge-Based Systems*, *259*. https://doi.org/10.1016/j.knosys.2022.110011

[19] Mahmoud, M. A., Md Nasir, N. R., Gurunathan, M., Raj, P., & Mostafa, S. A. (2021). The current state of the art in research on predictive maintenance in smart grid distribution network: Fault's types, causes, and prediction methods - a systematic review. *Energies*, *14*(16). https://doi.org/10.3390/EN14165078

[20] C, S. & Nimmagadda, P. (2024). Design of efficient alterable bandwidth FIR filter bank for hearing aid system. *E-Prime - Advances in Electrical Engineering, Electronics and Energy*, *7*. https://doi.org/10.1016/j.prime.2024.100478

[21] Maqbool, M., Sharma, V. K., & Kaushik, N. (2024). CNTFET-based SRAM cell design using INDEP technique. *E-Prime - Advances in Electrical Engineering, Electronics and Energy*, *7*. https://doi.org/10.1016/j.prime.2024.100477

Contact information:

Zishuo CHEN
Silesian College of Intelligent Science and Engineering,
Yanshan University, China

Jingfeng GUO
(Corresponding author)
School of Information Science and Engineering,
Yanshan University, China
E-mail: jfguo_ysu@163.com

Fengda ZHAO
School of Information Science and Engineering,
Yanshan University, China

Ruishan DU
School of Computer and Information Technology,
Northeast Petroleum University, China
Key Laboratory of Oil & Gas Reservoir and Underground Gas Storage Integrity Evaluation of Heilongjiang Province, Northeast Petroleum University, China

Lingdong MENG
Key Laboratory of Oil & Gas Reservoir and Underground Gas Storage Integrity Evaluation of Heilongjiang Province, Northeast Petroleum University, China